Formation, Interaction and Merger of an Active Region and a Quiescent Filament Prior to Their Eruption on 19 May 2007

L.A. Bone · L. van Driel-Gesztelyi · J.L. Culhane · G. Aulanier · P. Liewer

Abstract We report observations of the formation of two filaments – one active and one quiescent, and their subsequent interactions prior to eruption. The active region filament appeared on 17 May 2007, followed by the quiescent filament about 24 hours later. In the 26 hour interval preceding the eruption, which occurred at around 12:50 UT on 19 May 2007, we see the two filaments attempting to merge and filament material is repeatedly heated suggesting magnetic reconnection. The filament structure is observed to become increasingly dynamic preceding the eruption with two small hard X-ray sources seen close to the active part of the filament at around 01:38 UT on 19 May 2007 during one of the activity episodes. The final eruption on 19 May at about 12:51 UT involves a complex CME structure, a flare and a coronal wave. A magnetic cloud is observed near Earth by the STEREO-B and WIND spacecraft about 2.7 days later. Here we describe the behaviour of the two filaments in the period prior to the eruption and assess the nature of their dynamic interactions.

L.A. Bone · L. van Driel-Gesztelyi (✉) · J.L. Culhane
UCL – Mullard Space Science Laboratory, Holmbury St. Mary, Dorking, Surrey, RH5 6NT, UK
e-mail: lvdg@mssl.ucl.ac.uk

L. van Driel-Gesztelyi · G. Aulanier
LESIA, UMR 8109 (CNRS), Observatoire de Paris, 92195 Meudon Principal Cedex, France

L. van Driel-Gesztelyi
Konkoly Observatory of the Hungarian Academy of Sciences, Budapest, Hungary

P. Liewer
Jet Propulsion Laboratory, California Institute of Technology, MS 169-506, Pasadena, CA 91109, USA

1. Introduction

Filaments or prominences are formed of cool dense material suspended in magnetic fields in the hot corona. Although the mechanisms for filament formation are not fully understood, they are typically observed to form as relatively short structures that then merge to form new structures which can be hundreds of megametres long. Typically these merging filaments are of the same chirality or handedness (Martin and Echols, 1994; Schmieder *et al.*, 2004; Martens and Zwaan, 2001). There are a number of necessary conditions for filament formation, which include the formation of filaments along the polarity inversion line, the presence of a highly sheared overlying arcade, the existence of a filament channel, the presence of converging magnetic fields and magnetic flux cancellation. For a comprehensive review of filament formation, see Martin (1998). The axial field of the filament channel, filament and overlying arcade are always aligned and indicate the handedness or chirality of the filament.

In this paper we discuss observations of the interaction and apparent reconnection of two filaments. We use Hα data from the Kanzelhöhe, HASTA, Hida, Yunan and Huariou observatories to track the evolution, interaction and heating of the two filaments along with SOHO/MDI data to determine their magnetic orientation. STEREO/EUVI and *Hinode*/XRT data allow us to examine the evolution of the overlying field and the heating of the filament material through a series of reconnections. These filaments later erupt, in conjunction with a small flare and produce a complex CME observed as a magnetic cloud near Earth with STEREO/IMPACT. We discuss the likely signatures and mechanisms of the filament merging and the implications for the later eruption.

2. Observations

We have gathered extensive observations of the filament evolution and eruption from ground based Hα and from the satellite borne STEREO/EUVI and *Hinode*/XRT. We combine this with MDI data to determine the magnetic field configuration in the active region and the surrounding quiet Sun. The Hα images used in this paper come from many different observatories and were taken under varying seeing conditions. Furthermore, in these images the central wavelength may shift due to changes in ambient temperature; however, in the majority of cases, our interpretations do not rely on subtle properties of the images, because we are comparing different parts of the interacting filaments within the same image.

The SOHO/MDI line of sight magnetic field data are used to determine the magnetic field configuration in the active region and its surroundings. The sunspot group is relatively complex with a $\beta - \gamma - \delta$ classification involving more than one polarity inversion line and umbrae of different polarity close to one another within a single penumbra. Initially, as the sunspot group crosses the limb on 14 May, it has a fairly simple bipolar configuration. Within 24 hours (starting at ≈08:03 UT on 15 May) further emergence of flux on the western side of the AR has increased the complexity of the active region, while the leading polarity is now positive (non-Hale). It is along the polarity inversion line between the leading positive polarity and the main negative polarity that the active region filament forms within less than a day: by 01:55:45 UT on 16 May dark fibrils extending toward the north-west of the active region are seen in the STEREO/EUVI He II 304 Å data, but as early as at 23:55:45 UT on the 15th some signs of activity (brightenings) are visible along the future filament's channel. This initial filament undergoes eruption starting at ≈17:45 UT on 16 May (see secchi.lmsal.com/EUVI/MOVIES_ANAGLYPH/20070513_304.mov). The re-formation of filament structures begin on the 17 May (Figure 1). The two panels of the figure indicate that

Figure 1 Hα filament observations on 17 May 2007 showing the initial formation of the active region filament (a) and its extension to the north-west (b). The image in (a) is from the Kanzelhöhe Solar Observatory, while the image from the SMART Hα telescope at the Hida Observatory (b) was taken over nine hours later.

11:45:27 UT   21:06:53 UT
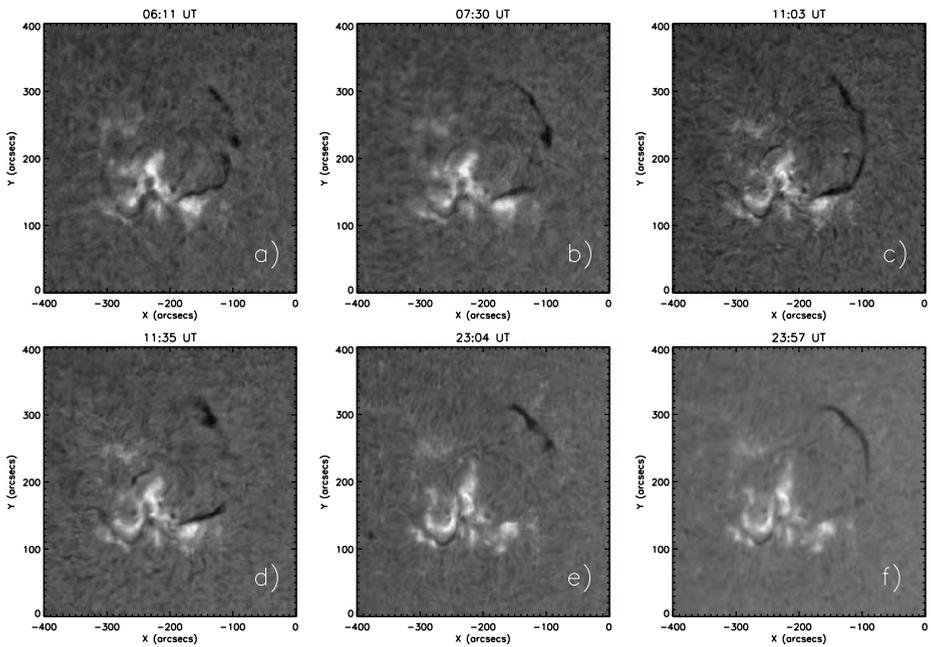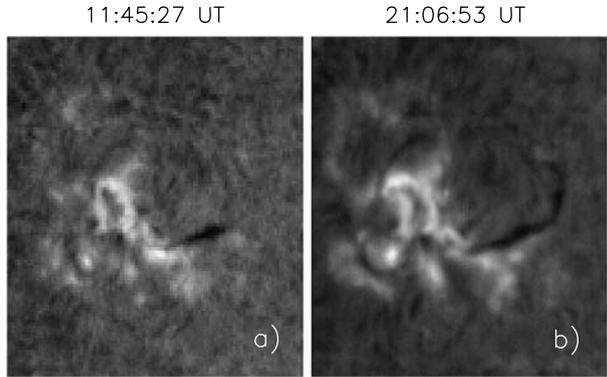
Figure 2 Hα filament observations on the 18th May showing filament merging and partial disappearance. Panels (a) – (d) are from the Kanzelhöhe Solar Observatory, (e) and (f) are from the SMART Hα telescope at the Hida observatory. All frames have been de-rotated to 06:11 UT on the 18th May.

the filament more than doubled in length within nine hours. Even though both the seeing and possibly even the central wavelength of the Hα filter differ in these two images, the elongation of the filament is beyond doubt. On 18 May (Figure 2, panel (a)), we see the first appearance of filament material along the same polarity inversion line outside of the active region in the quiet Sun. The location of the filament material in relation to the magnetic field configuration can be seen in Figure 3.

Analysis of the MDI data over the time period 17 May – 19 May shows the cancellation of magnetic flux occurring in both the active and quiescent parts of the filament channel as an almost continuous process. Figure 4 shows some of the flux cancellation events during

Figure 3 MDI magnetogram showing the original sunspot bipole (bipole 1) and the bipole which later emerged (bipole 2). The active region filament lies between the leading (positive) polarity and the central negative polarity. The quiet Sun filament preceding the disappearance at 11:45 UT is rotated to the same time and overlayed, showing its location along a polarity inversion line between positive and negative polarities outside the active region (black contours).
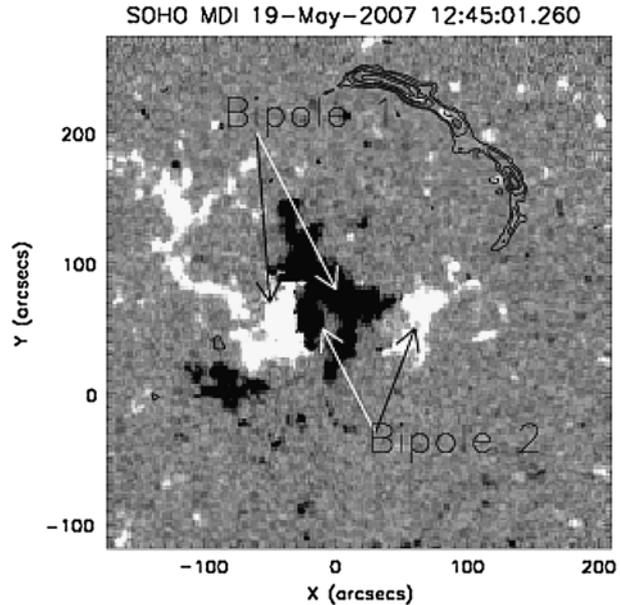
this period. We see major flux cancellation along the western inversion line in the AR (Figure 4a), and small fragments of negative flux cancelling with the positive flux at the edge of the active region (Figures 4a and b). The negative fluxes in cancellations over the quiet Sun in Figures 4a and b may originate at bipole 1 (shown in Figure 3), which is decaying. These small pieces of negative flux then cancel with the predominantly positive magnetic flux of the surrounding quiet Sun along the filament channel.

Using an MDI movie with images de-rotated to the time of the central meridian passage of the AR we identified cancellation sites along the entire filament channel. Then we measured the magnetic flux of the minority polarity of the most prominent cancelling elements and calculated a mean cancellation rate over the cancellation period. The cancellation rate was found highest along the AR inversion line ($7.5 \times 10^{19} - 1.7 \times 10^{20}$ Mx day^{-1}) over the period of 16 May 22:27 UT to 19 May 17:39 UT, but even along the quiescent filament channel we found considerable rates over the period of 17 May 08:03 UT to 19 May 00:03 UT ($3.4 \times 10^{19} - 1.4 \times 10^{20}$ Mx day^{-1}). Some of the episodes of flux cancellation on the 17, 18 and 19 May coincide with observed heating of the filament structure and increasing instability. These occurrences are summarised below.

For a number of hours after the emergence of the filament structure in the quiet Sun the two filaments appear to be separate (see panels (a) and (b) of Figure 2). The first time the filament can be seen as a continuous structure is in the third of the Hα images from Kanzelhöhe observatory taken at 11:03 UT on 18 May (panel (c)). Shortly after this time the central body of the filament disappears from the Hα band (panel (d)), while the remaining part of the active filament is absent by 23:04 UT (panel (e)). However, a partial reappearance is evident at 23:57 UT (panel (f)) in the second of the frames from the SMART telescope. This would suggest that if the material is being heated, the temperature is too low for the filament to be seen in emission in even the EUVI 304 Å band. Nevertheless it is entirely possible that the changes in filament structure seen in panels (d), (e) and (f) are due to motion of the filament material in the line of sight direction. However EUV and X-ray emission from the plasma would indicate that the temperature has increased to at least 0.08 MK for
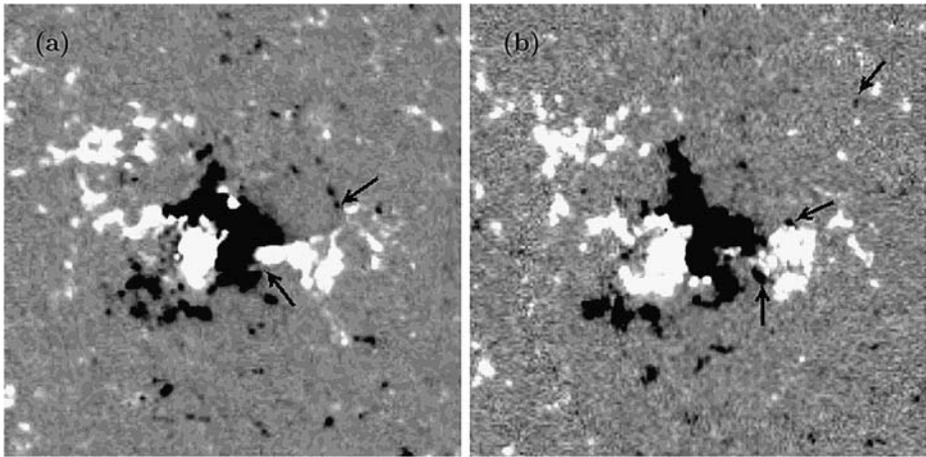
Figure 4 MDI magnetograms (a) on the 17 May at 11:15 UT and (b) on the 18 May at 19:08 UT showing flux cancellation sites along the western AR inversion line, where the active region filament lies, and in the quiet Sun along the filament channel of the quiescent filament.
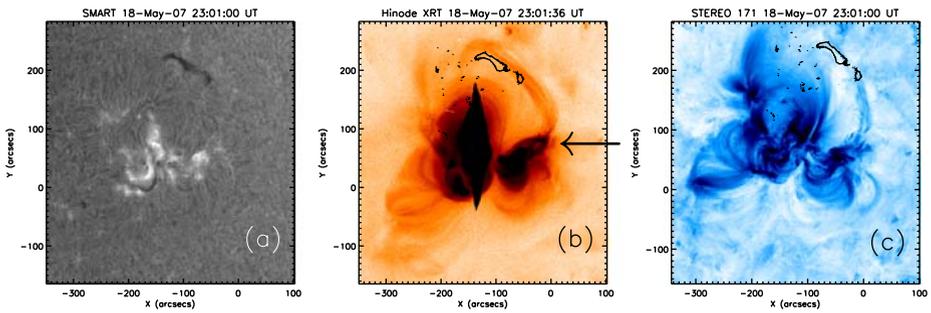
Figure 5 (a) Hα image from the Hida observatory on 18 May showing the disappearance of the lower part of the filament. (b) Cusp structure of low lying loops towards the NW (indicated by an arrow) and extended X-ray emission along the filament channel seen by *Hinode*/XRT. (c) Extended emission is also evident in the STEREO/EUVI images.

He II 304 Å. Thus between 11:03 UT on 18 May when the two filaments first appear as one structure and the eventual eruption of the filament 27 hours later the material is observed to undergo a number of periods of heating, implying that energy is being supplied, presumably through the reconnection and reconfiguration of the field. We will now discuss a number of these periods of heating in detail.

18 May 23:00 – 23:30 UT

In this heating episode the entire lower half (active region) part of the filament disappears from the Hα passband (Figure 5a). We see a cusp structure form in XRT images of the low lying loops between the leading positive and trailing negative polarity and a long structure brightens along the filament channel in the XRT image shown in Figure 5b. This structure is closely co-spatial with the filament material seen in Hα as is shown in Figure 5a, implying
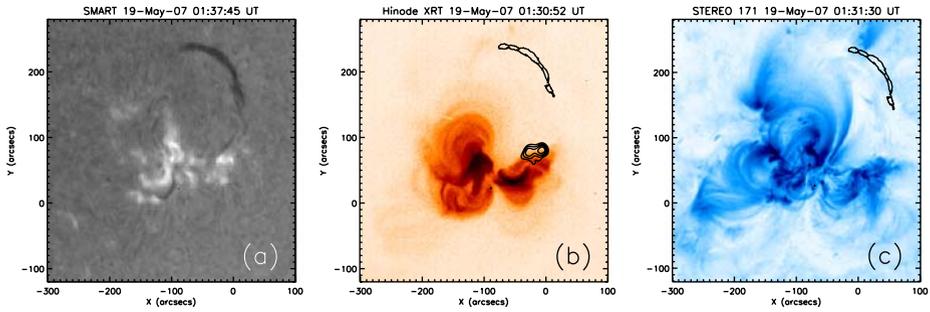
Figure 6 Hα image from Hida observatory showing the disappearance of the lower part of the filament (a), contours for a small RHESSI source over an XRT image (b) and heated material in STEREO/EUVI (c).

that material along the filament channel is being heated to at least 3 MK at this time. Extended loop structures are also observed in all four STEREO/EUVI filters (the 171 Å filter image is shown in Figure 5c).

19 May 01:30 – 02:00 UT

From 01:30 UT we again see the lower part of the filament disappear from Hα (Figure 6a). There is little or no extended structure in X-rays (Figure 6, panel (b)), however the low lying loops observed with XRT are once again visible. During this event we also see weak emission with the RHESSI spacecraft below 12 keV (panel (b)). This implies that either the plasma is heated to relatively high temperatures, or that a weak non-thermal accelerated electron beam is present. The absence of soft X-ray emission suggests that the latter possibility is more likely. A similar RHESSI signature was observed in an active filament by Williams *et al.* (2009). In that case there was no conclusive evidence for the filament erupting, but both expansion and twisting were observed. Emission is also seen in EUVI 171 Å in the lower (active region) part of the filament channel, but not in the higher temperature filters, implying that this plasma is heated to no more than ≈1 MK (panel (c)).

19 May 04:30 – 06:00 UT

Two separate incidents of heating occur within this time interval, one of which is discussed below. They follow a similar pattern to that observed in the previous episodes. At 03:00 UT the Yunnan patrol image (Figure 7) shows what appears to be two separate filaments, active region and quiescent, though a faint bridge may exist between them that is difficult to discern due to seeing quality. A little later between 04:00 UT and 04:39 UT saturated images from the Huariou observatory show a strengthening of the link leading to an apparent merger (Figures 7b and c). However by 04:36 UT the active region filament essentially disappears and the connection to the quiescent filament is entirely absent (Figure 7d). Although the evidence from disappearance and reappearance in the Hα images may not be conclusive, the corresponding evidence for heating of some of the filament material as shown in Figure 8 is quite clear. In an XRT image taken at 04:30 UT, soft X-ray emission is seen to replace most of the cool, absorbing AR filament material. However a fainter X-ray emitting structure appears to co-exist with the quiescent component of the Hα filament. Finally emission at 171 Å ($T \approx 1$ MK) is apparent in a TRACE image (Figure 8). This structure is possibly slightly above the X-ray emission indicating a complex variation of the heating process with height.
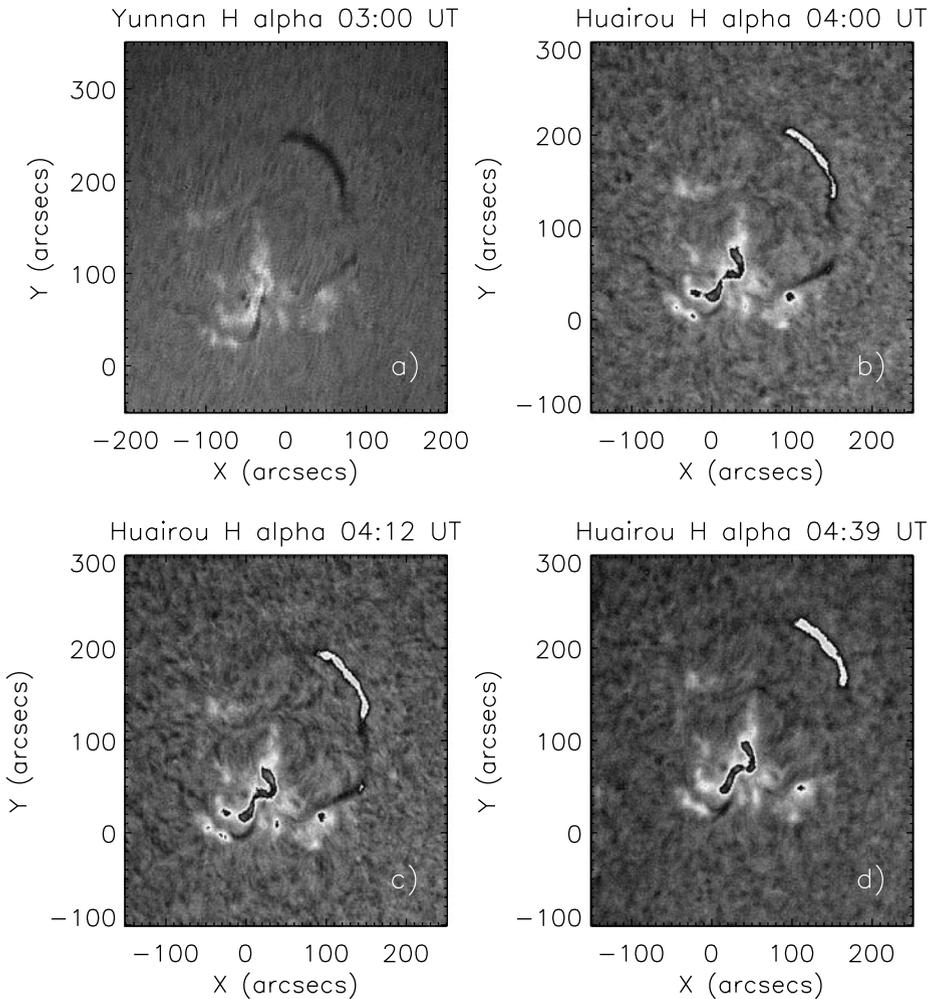
Figure 7 Hα images from Yunnan (a) and Huairou (b, c) show a strengthening of the link leading to an apparent merger followed by a partial disappearance (d).

Final Heating and Eruption

The final disappearance of the filament from the Hα data progresses in several stages. In the hours prior to the eruption the material appears very dynamic, with the filament structure fluctuating and with sections of the filament appearing and disappearing. Figure 9 shows this in several ways by examining a section of the filament over the period of the Kanzelhöhe data set on 19 May. The chosen section of filament is indicated in Figure 10. The top panel in Figure 9 is an integrated light curve which shows fluctuation in intensity. The middle panel shows an integration in X over a section of the filament which illustrates the variation in the north–south direction, and indicates the repeated heating and cooling of the middle section of the filament. The bottom panel is an integration in Y and shows the movement of the filament in the east–west direction.
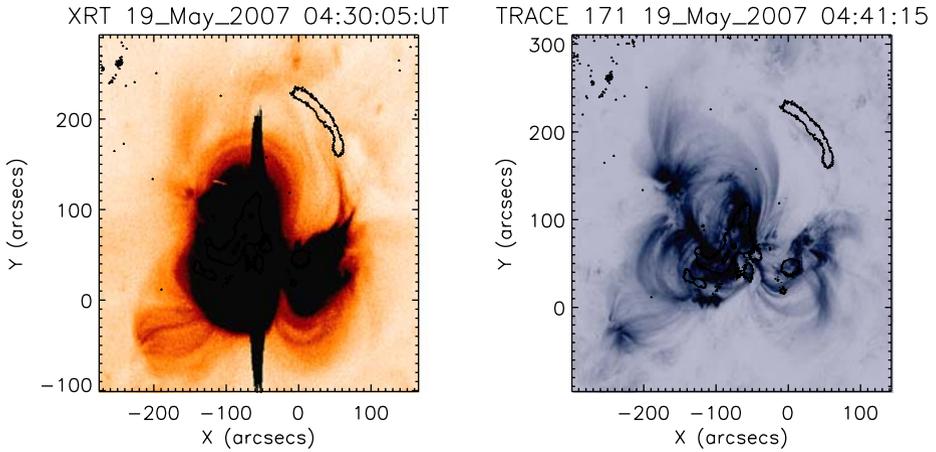
Figure 8 Heated material in XRT and TRACE with the Hα filament structure overlayed.
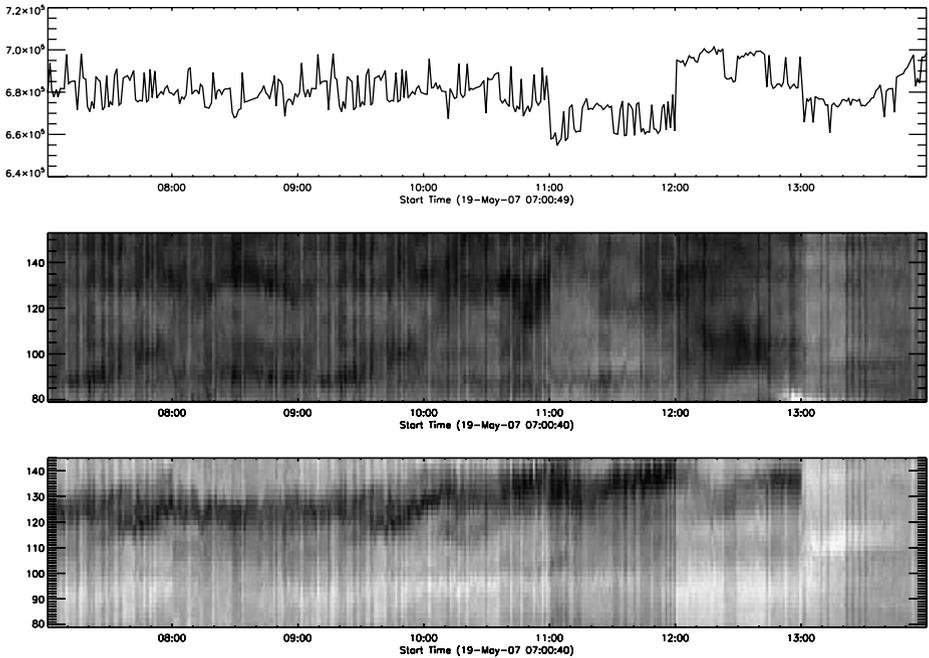
Figure 9 Lightcurve and stackplots in *X* and *Y* showing the variation in the filament in the Kanzelhöhe data set on the 19th May. The top panel shows the summed emission, the middle is the variation in *Y* intensity and the bottom is the variation in *X* intensity. The images were de-rotated to the time of the initial frame before being summed.

At 10:38 UT on 19 May a complete filament exists (Figure 11a). Around 12:17 UT the lowest extension of the filament into the active region begins to disappear (Figure 11b). We then see the entire lower part of the filament, located in the active region disappear between 12:30 and 12:44 UT. There is a delay of several minutes before the upper part, which was

KANZELHOEHE HALPHA PATROL TM1010 6563 19−May−2007 12:27:48.000 UT
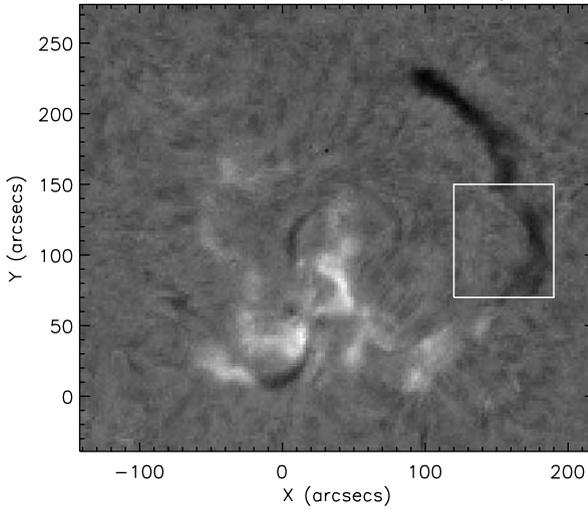
Figure 10 Region of the filament examined in the previous figure.
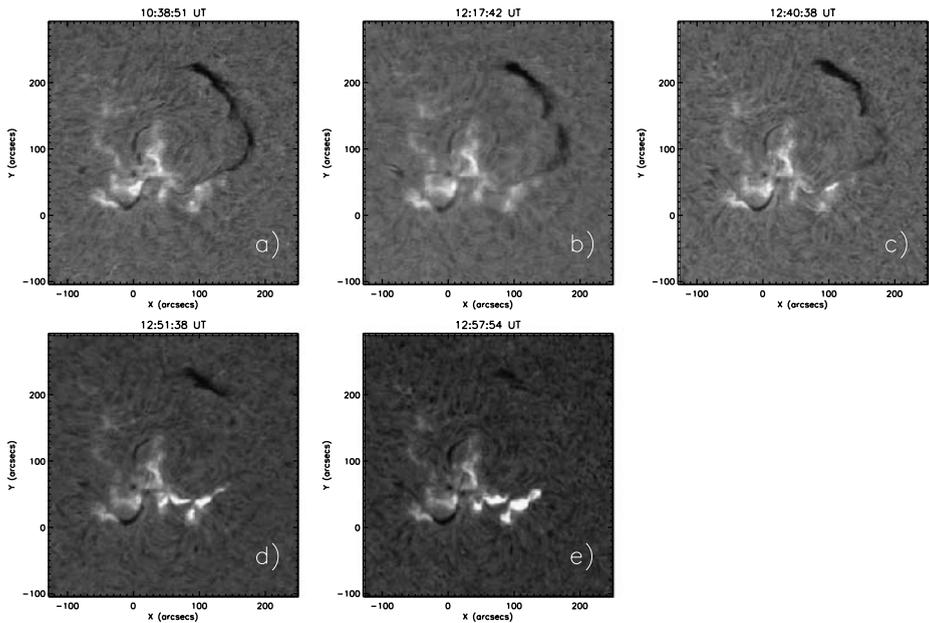
Figure 11 The evolution of the filament material in Hα prior to and during the eruption on 19 May. All images are de-rotated to 10:06 UT on 19 May.

originally the separate quiet Sun filament begins to disappear between 12:44 and 12:57 UT (Figures 11c and d). As the filament disappears from the observations in Hα line centre, we see it clearly in both the red and blue wings of the Hα line, suggesting that the material is moving at a velocity of 20 km s^{-1} (Figure 12). The upflows, shown in the blue wing images
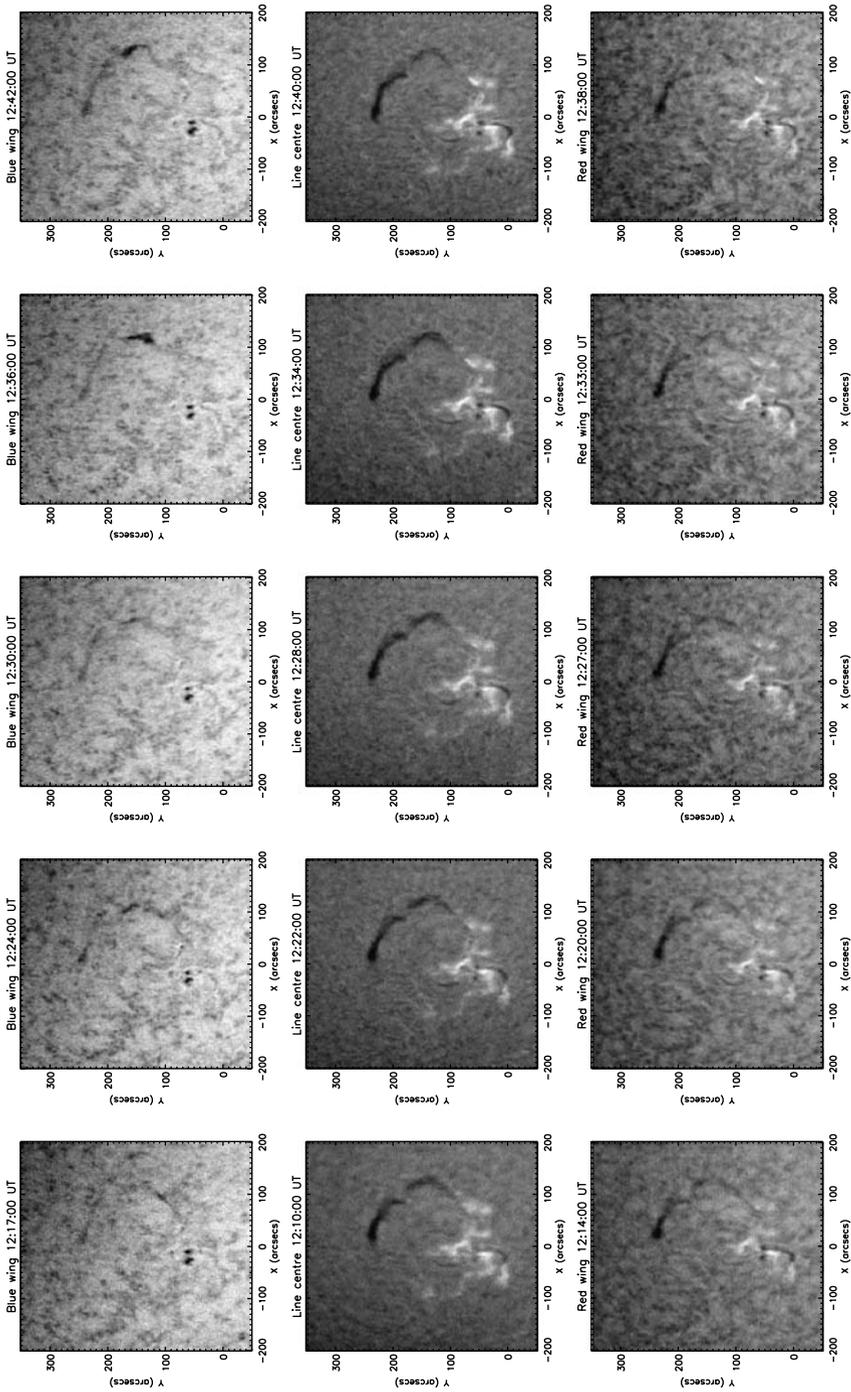
Figure 12 Hα observation from HASTA showing the filament in the red wing, line centre and blue wing, immediately preceding the eruption.

EUVI 171 Angstrom evolution
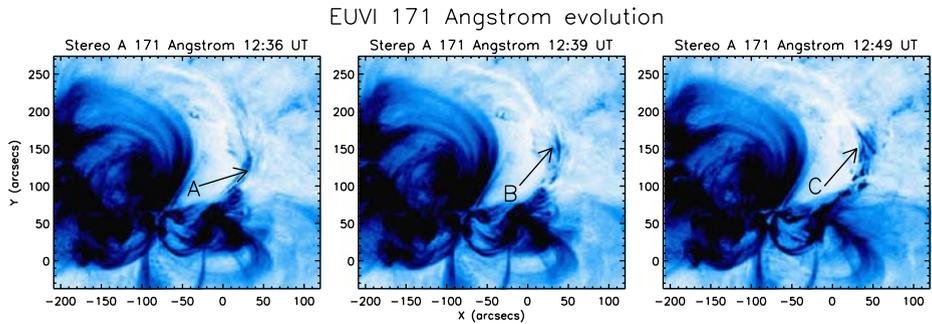
Figure 13 Contemporaneous with the lower filament material disappearing in Hα we see a long loop brightening in the STEREO/EUVI 171 Å passband (leftmost panel, arrow A). Short structures form (middle panel, arrow B) and brighten (right panel, arrow C) across the filament polarity inversion line.

begin at the active region footpoint of the filament as early as 12:17 UT and progress along the filament to almost its entire length in the image closest to the eruption at 12:42 UT. The downflows in the red wing images persist at the quiescent end of the filament, farthest from the AR. These flows are consistent with the observed asymmetric nature of the eruption, with the AR end of the filament leading, followed by the slower quiescent part.

We also observe material in emission in EUV with STEREO, where we see long loop structures brighten in EUVI 171 Å as before, as well as short structures overlying the polarity inversion line (Figure 13, arrows B and C), these structures may be material in the dips of the flux rope which is being strongly heated prior to eruption.

With XRT we initially see brightening in the sigmoidal loops in the active region followed by brightening of material along the whole filament channel, which disappears as the filament erupts (Figure 14).

3. Discussion

In this section we summarise the processes involved in the formation of the filaments and the role of magnetic helicity. Following formation, we describe the progressive process of interaction and merging that takes place. This phase ends with a last heating episode followed by merger and the eruption whose nature we outline.

3.1. Formation and Helicity of the Filaments

On one hand, the channel of the southern active region filament initially forms along the new inversion line that develops between the leading positive polarity of a non-Hale bipole (referred to as Bipole 2 in Figure 3) which started emerging on 15 May, and the leading negative polarity of the pre-existing active region (referred to as Bipole 1 in Figure 3).

On the other hand, the negative polarity part of Bipole 1 is continuously decaying. This decay manifests itself through flux dispersion, in the form of moving magnetic features. The latter continually stream out of the spot to the north-west into the quiet Sun, which originally had a dominantly positive polarity. This results in an extended inversion line along which the quiescent filament started forming on 15/16 May. This initial filament erupted at ≈17:45 UT on 16 May. We followed the re-formation of filament structures from 17 May. As postulated by Martens and Zwaan (2001): "The formation of a filament . . . is driven by
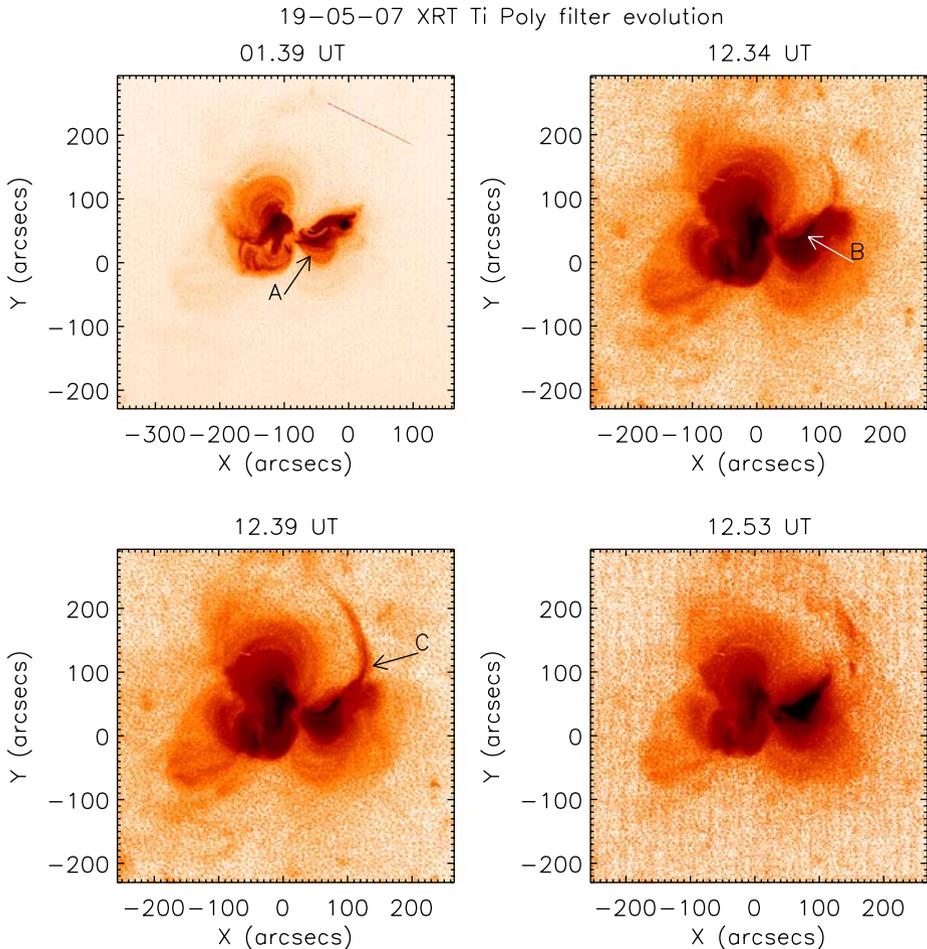
Figure 14 XRT Ti poly filter images of the active region. Initially we see a forward S-shaped structure where the flare later occurs (top left, indicated by arrow A). As the lower filament material disappears we see a brightening in X-rays (top right, indicated by arrow B), followed by the formation of a long loop structure (bottom left, arrow C) and finally the flaring loops form (bottom right).

flux convergence and cancellation, which produces looplike filament segments with a half-turn. Filament segments of like chirality may connect and form long quiescent filaments. Such filaments are stabilised through footpoint anchoring until further cancellation at the footpoints causes their eruption. The eruption restores the original filament channel so that filament formation may resume immediately." Though we observe "act II" of this filament formation and merging following the eruption on 16 May, the characteristic processes should be very similar to those that occurred during the primary formation.

The magnetic cancellation rate we found along the forming active region and quiescent filaments was $7.5 \times 10^{19} - 1.7 \times 10^{20}$ Mx day^{-1} = $3.1 - 7.1 \times 10^{18}$ Mx hr^{-1} along the AR inversion line, an order of magnitude lower than observed by Chae *et al.* (2001) under a forming filament, but a factor of $3 - 7$ higher than obtained by Contarino, Romano, and Zuccarello (2006) prior to filament activation. Even along the quiescent filament channel we

found considerable cancellation rates of $3.4 \times 10^{19} - 1.4 \times 10^{20}$ Mx day^{-1} = $1.4 - 5.8 \times 10^{18}$ Mx hr^{-1}, which are all higher than characteristic mean cancellation rates found for the quiet-Sun (2.4×10^{18} Mx day^{-1} or 10^{17} Mx hr^{-1}; Harvey, 1985). Li *et al.* (2008) showed that the total magnetic flux of AR 10956 decreased by $\approx 17\%$ during the two days preceding the filament eruption of the 19 May. However, most of the flux cancellations took place along the central neutral line in the AR, and cancellations related to the formation and merger of the two filaments we study only represented 6% of the flux change over this two-day period.

The polarity inversion lines of both filaments actually join on the west side of the active region, even though both filaments are distinct from one another for about 30 hours. Between 17 May and 19 May, the coronal magnetic stress in both filaments increased, due to flux cancellation processes (van Ballegooijen and Martens, 1989; Chae *et al.*, 2001) below the quiescent filament (see Figure 4) and to cancellation coupled with slow shearing of the active region filament that resulted from the proper motion of the leading polarity of Bipole 2. These two filaments, which share a common inversion line, interact, merge and finally erupt on 19 May. This raises the question of the underlying mechanisms for these three processes.

A key aspect which determines the fate of interacting filaments that share the same inversion line is the direction of their axial fields, which turn out to correspond to the sign of their magnetic helicity when the large-scale configuration is bipolar, as it is the case here (see Figure 3). It has been shown theoretically by DeVore, Antiochos, and Aulanier (2005) and Aulanier, DeVore, and Antiochos (2006) in the framework of the so-called sheared arcade model, as well as observationally by Schmieder *et al.* (2006), that when two such filaments have the same helicity sign, they can merge through a series of finite-B coronal reconnections as the shear increases with time.

Let us consider first the active region filament. The orientation of chromospheric fibrils on its northern edge as observed in Hα is suggestive of a sinistral chirality for the filament (following Martin (1998)). This chirality is consistent with a positive helicity sign, in accordance with linear force-free field models for filaments (Aulanier and Démoulin, 1998) as well as with the forward-S shape of the overlaying coronal loops as observed with *Hinode*/XRT (see Figure 14 at 01:39 UT). Now we consider the quiescent filament. On its eastern side, the orientation of the fuzzy Hα fibrils is the same as that of the very thin and bright EUV threads as observed with STEREO/EUVI (see Figure 13). If one considers the latter as being a signature of hot material in the low altitude magnetic dips of a weakly twisted coronal flux tube (which also develop in the sheared arcade model), then these features also correspond to a positive magnetic helicity for this filament. Since this is a N-hemisphere region, helicity is typically negative. Thus these two filaments do not follow the statistical rules for the helicity pattern of solar features (Pevtsov, Canfield, and Metcalf, 1995).

Typical coronal field lines and chromospheric fibrils for both distinct filaments are sketched in Figure 15a. Here the differentially sheared (or weakly twisted) S-shape filament field lines are drawn in orange and cyan, and overlaying coronal arcades are drawn in red and blue.

3.2. Interaction and Merging of the Filaments

Shortly after both filaments have formed, multiple interactions take place one after the other between the two sections. Evidence of these episodes includes the appearance of transient hot material in and around the joint filament channel, as observed by STEREO/EUVI and *Hinode*/XRT. During these heating periods, Hα absorbing material disappears from the interfacing ends of both filaments, which later not only reappear, but also develop along the
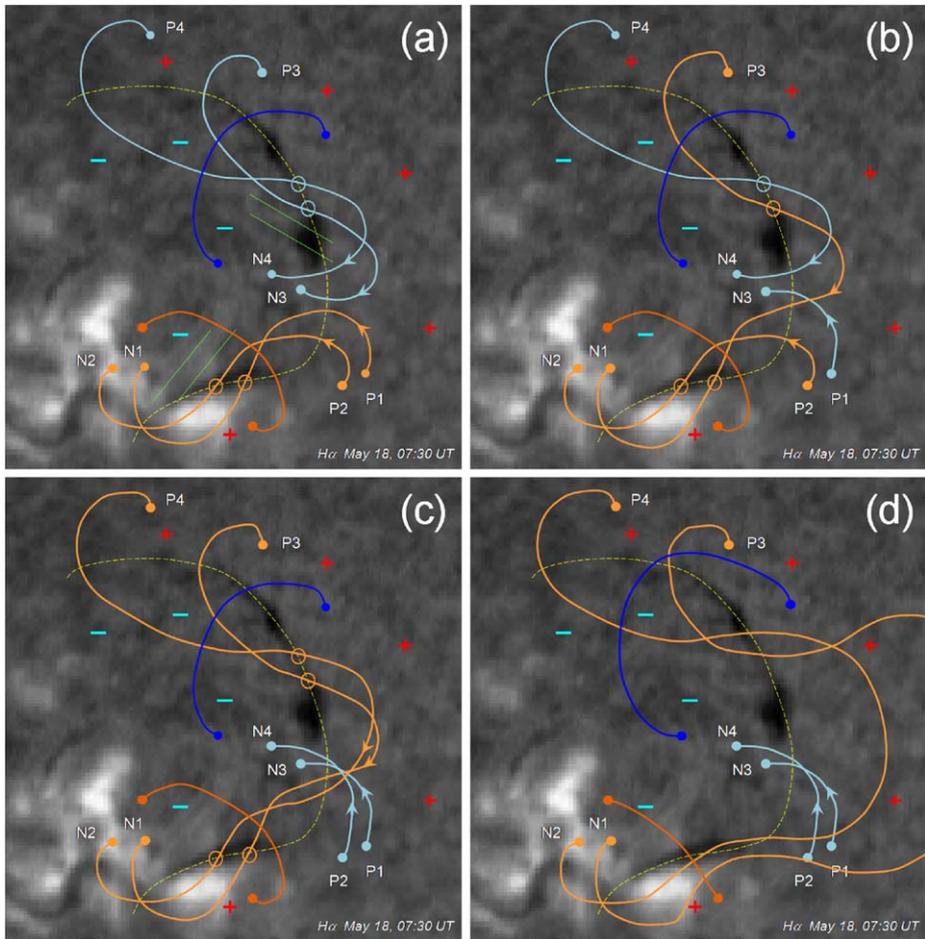
Figure 15 Cartoon model showing the evolution of field lines due to the merging of the two filaments. Initially (a) the filaments are two separate structures which, through reconnection, form long interlinking field lines and short, transverse structures (b and c), which eventually become unstable and erupt (d).

filament channel so as to produce a single merged filament. The merged filament only lasts from a few tens of minutes to more than one hour, until a new heating episode starts. We argue that these episodes correspond to a sequence of coronal reconnections between the two progenitor filaments. Such reconnections must not only result in plasma heating and conductive transport along the inversion lines, but also in the formation of new interlinking magnetic connections between both filaments. In an idealised and symmetric MHD model, it has been shown that the early stages of such a process produce transient coronal magnetic dips between both interacting filament (DeVore, Antiochos, and Aulanier, 2005; DeVore and Antiochos, 2006). In a configuration as complex as the one observed here, such interaction episodes are likely to be numerous. Therefore we argue that the observed transient heating and merging episodes were signatures of this physical process. The same MHD models show that in the last stages of filament interaction, a single magnetic flux tube of complex topology is produced, which does possess stable magnetic dips in the middle and so can re-

sult in a stable single filament. We therefore believe that our filaments experience a long and difficult merging process, as shown by the variability of the Hα patterns prior to eruption displayed in Figure 9, for the subsection of the filament shown in Figure 10. This process eventually ended on 19 May, just before the eruption at 12:51 UT.

The slow merging process is sketched in Figure 15a–c. This conceptual model results in new long interlinking filament field lines, whose twists must be larger than the twist in each of the pre-reconnection S-shape field lines. It must also result in the formation of heated loops below the merging region, drawn in cyan. The latter may be related to the RHESSI signature observed during one of the heating episodes on 19 May at 01:30 UT (see Figure 6b). This reconnection, which eventually results in the full merging (see Figure 15c) is in accordance with the tether-cutting model of Moore (2000), in which reconnection between sheared field lines produces an underlying small loop (blue) and an overlying long sheared loop (orange).

3.3. Eruption of the Merged Filament

As soon as the merging has been achieved, a last heating episode launches a conduction front northward along the quiescent filament, as observed by Hinode/XRT (see Figure 14). This heating also has a counterpart in the form of EUV 304 Å loop brightenings located at the eastern end of the active region filament, as observed with STEREO/EUVI (see the electronic supplement stereo_304.mov (doi:10.1007/s11207-009-9363-4) as well as the Figure 9 of Liewer *et al.* (2009)). These joint brightenings are very important, in the sense that they prove that the filament has finally succeeded in fully merging by that time. This last heating episode also results in the formation of a non-moving X-ray bright point at 12:50:21 UT (see Figure 14) below the site of merging, which is exactly co-temporal with the start of the eruption, as far as the XRT time-resolution allows us to determine.

The time evolution of line of sight motions, as observed with HASTA in Hα (see Figure 12) actually shows the rise of the northern part of the filament 10 minutes before the eruption starts, with corresponding downflows at the north-eastern footpoint. These flow patterns are highly suggestive that the top of the erupting flux tube is indeed between the two former progenitor filaments, and therefore that their resulting merged flux tube is the erupting feature. They are also consistent with the stereoscopic reconstruction of the eruption itself, which shows that the north-east part of the filament became more and more vertical with respect to the photosphere (Liewer *et al.*, 2009), thus allowing downward motions of dense material along the erupting field lines.

Following our sketch model with these observational constraints, we argue that the bright point was caused by the reinforcement of the reconnection that produced flare-type loops and earlier cusp structures. We also conjecture that the eruption was a direct consequence of the formation of a longer and more twisted flux tube (resulting from the merging of the two filaments), which could easily expand westward and toward higher altitudes, due to the horse-shoe shape of the inversion line and to the concentration of magnetic energy on the south-east side of the filament (within the active region). In other words, the merged filament would naturally expand toward the weakest field regions. Still, our geometrical analysis does not allow us to identify which mechanism actually produced the fast acceleration of the eruption. This eruption is sketched in Figure 15d.

Veronig, Temmer, and Vršnak (2008) have argued that this event was due to the separate eruption of both filaments, supported by the observation of two CMEs of different velocities with LASCO/C2 and STEREO/COR1. This picture disagrees with our merger and eruption scenario. Furthermore Liewer *et al.* (2009) have shown that the early disappearance of the

active region filament at 12:42 UT, about 10 min prior to the eruption, coincided with the appearance of bright emissive threads in EUVI 304 Å. This indicates that the fading of the southern part of the filament was actually due to plasma heating, and not to a first distinct eruption. Although two CME sections were observed with different velocities, this is not inconsistent with the eruption of a single merged filament. Since the south-east section was rooted in sunspot-related strong magnetic fields, it is likely that the driving Lorentz forces were stronger here than in the north part of the filament channel since the latter was located in the quiet Sun. This asymmetry in the distribution of the magnetic fields can account for an asymmetric eruption in which the southern section could rise faster than its north counterpart. Given the line of sight integration inherent in coronographic observations, as well as the angular efficiency of Thomson scattering which results in emphasis on different plasma elements by SOHO and STEREO, these two sections of the same CME could easily be misinterpreted as two separate features. Thus the observations are not in conflict with our model.

4. Conclusions

We report observations of the re-formation of two filaments – one active and one quiescent, and their subsequent interactions prior to eruption. Following an eruption on 16 May 2007, the active region filament re-formed on 17 May followed by the quiescent filament about 24 hours later. The two filaments made several attempts to merge and filament material is repeatedly heated suggesting magnetic reconnection.

The scenario leading up to the eruption involves a series of reconnections between the two filament sections that in turn leads to a build-up of shear and the formation of long linking loops between the two sections. The build-up of shear, along with the removal of overlying field by magnetic flux cancellation, leads to the increasing instability and eventual eruption of the two filament sections. The filament structure is observed to become increasingly dynamic preceding the eruption. The final eruption on 19 May proceeds in two parts, with initially the active region section of the filament erupting, followed by the quiescent section, causing a complex CME, a flare and a coronal wave.

The role of the merger was to produce a long and highly stressed flux tube, with its middle part being located right below a weaker coronal magnetic field region, thus allowing the eruption of the flux tube through this weakly confining region. Without the merging, each separate filament would have been more confined by their overlaying arcades, and some other mechanisms than the merging would have been required for them to erupt.

References

Aulanier, G., Démoulin, P.: 1998, 3-D magnetic configurations supporting prominences. I. The natural presence of lateral feet. *Astron. Astrophys.* **329**, 1125–1137.

Aulanier, G., DeVore, C.R., Antiochos, S.K.: 2006, Solar prominence merging. *Astrophys. J.* **646**, 1349–1357. doi:10.1086/505020.

Chae, J., Wang, H., Qiu, J., Goode, P.R., Strous, L., Yun, H.S.: 2001, The formation of a prominence in active region NOAA 8668. I. SOHO/MDI observations of magnetic field evolution. *Astrophys. J.* **560**, 476–489. doi:10.1086/322491.

Contarino, L., Romano, P., Zuccarello, F.: 2006, Cancelling magnetic feature and filament activation. *Astron. Nachr.* **327**, 674. doi:10.1002/asna.200610619.

DeVore, C.R., Antiochos, S.K.: 2006, Sympathetic breakout coronal mass ejections. *Bull. Am. Astron. Soc.* **38**, 236–236.

DeVore, C.R., Antiochos, S.K., Aulanier, G.: 2005, Solar prominence interactions. *Astrophys. J.* **629**, 1122–1134. doi:10.1086/431721.

Harvey, K.L.: 1985, The relationship between coronal bright points as seen in He I Lambda 10830 and the evolution of the photospheric network magnetic fields. *Aust. J. Phys.* **38**, 875–883.

Li, Y., Lynch, B.J., Stenborg, G., Luhmann, J.G., Huttunen, K.E.J., Welsch, B.T., Liewer, P.C., Vourlidas, A.: 2008, The solar magnetic field and coronal dynamics of the eruption on 2007 May 19. *Astrophys. J.* **681**, L37–L40. doi:10.1086/590340.

Liewer, P.C., de Jong, E.M., Hall, J.R., Howard, R.A., Thompson, W.T., Culhane, J.L., Bone, L., van Driel-Gesztelyi, L.: 2009, Stereoscopic analysis of the 19 May 2007 erupting filament. *Solar Phys.* **256**, 57–72. doi:10.1007/s11207-009-9363-4.

Martens, P.C., Zwaan, C.: 2001, Origin and evolution of filament-prominence systems. *Astrophys. J.* **558**, 872–887. doi:10.1086/322279.

Martin, S.F.: 1998, Conditions for the formation and maintenance of filaments (invited review). *Solar Phys.* **182**, 107–137. doi:10.1023/A:1005026814076.

Martin, S.F., Echols, C.R.: 1994, An observational and conceptual model of the magnetic field of a filament. In: Rutten, R.J., Schrijver, C.J. (eds.) *Solar Surface Magnetism*, 339.

Moore, R.: 2000, In: Murdin, P. (ed.) *Solar Prominence Eruption*, *Encyclopedia of Astronomy and Astrophysics*. doi:10.1888/0333750888/2282.

Pevtsov, A.A., Canfield, R.C., Metcalf, T.R.: 1995, Latitudinal variation of helicity of photospheric magnetic fields. *Astrophys. J.* **440**, L109–L112. doi:10.1086/187773.

Schmieder, B., Mein, N., Deng, Y., Dumitrache, C., Malherbe, J.M., Staiger, J., Deluca, E.E.: 2004, Magnetic changes observed in the formation of two filaments in a complex active region: TRACE and MSDP observations. *Solar Phys.* **223**, 119–141. doi:10.1007/s11207-004-1107-x.

Schmieder, B., Aulanier, G., Mein, P., López Ariste, A.: 2006, Evolving photospheric flux concentrations and filament dynamic changes. *Solar Phys.* **238**, 245–259. doi:10.1007/s11207-006-0252-9.

van Ballegooijen, A.A., Martens, P.C.H.: 1989, Formation and eruption of solar prominences. *Astrophys. J.* **343**, 971–984. doi:10.1086/167766.

Veronig, A.M., Temmer, M., Vršnak, B.: 2008, High-cadence observations of a global coronal wave by STEREO EUVI. *Astrophys. J.* **681**, L113–L116. doi:10.1086/590493.

Williams, D.R., Harra, L.K., Brooks, D.H., Imada, S., Hansteen, V.H.: 2009, Evidence from EIS for axial filament rotation before a large flare. *Publ. Astron. Soc. Japan* **61**, 493–497.